15

Optical Properties and Electromagnetic Wave Field Localization in a System of 2D Photonic Crystal Rectangular Resonant Cavities with Electromagnetic Coupling

© K.G. Elanskaya[1], A.I. Sidorov[1,2]

[1] Saint Petersburg Electrotechnical University „LETI", Saint Petersburg, Russia
[2] ITMO University, St. Petersburg, Russia

e-mail: sidorov@oi.ifmo.ru

The spectral properties and electromagnetic field distribution in a single photonic crystal resonator, as well as in systems of two and three coupled 2D photonic crystal rectangular resonant cavities, were studied using computer simulation methods. It is shown that under resonance conditions, significant localization of the electromagnetic wave field occurs in the resonant cavities. The quality factor of a system with three coupled photonic crystal resonant cavities can reach up to 3000. Electromagnetic interaction between the coupled resonant cavities leads to Fano resonances observed in resonant spectral bands.

Keywords: photonic crystal, resonant cavity, electromagnetic field, Fano resonance.

DOI: 10.61011/EOS.2025.09.62309.7703-25

Introduction

Photonic crystals (PCs) are widely used in various fields of optics and photonics [1,2]. They can serve as optical filters [3], demultiplexers [4], optical switches and logic gates [5,6], and polarization converters [7] in integrated optical devices. The sensitivity of PC optical characteristics to environmental influences makes them promising for various optical sensors, such as chemical and biosensors [8,9], mechanical parameter sensors [10], temperature sensors [11,12], etc.

One-dimensional (1D) and two-dimensional (2D) PCs are promising for integrated optics and sensorics. Optical components based on 1D and 2D PCs, such as waveguides and resonant cavities, have unique properties. They are compact and enable size reduction of integrated optical devices. Fabrication of 1D and 2D PCs is technologically simpler than 3D PCs, as photolithography alone can be used. 2D PC waveguides and resonant cavities integrate well with integrated optical devices [13]. They can also be used in microfluidic chips [14].

A key advantage of 2D PC resonators is strong localization of the electromagnetic wave field in the resonant cavity under resonance conditions. This effect can enhance sensitivity in chemical and biosensors based on Raman scattering [15]. The formation of electromagnetic coupling between 2D PC resonant cavities opens new possibilities for photonic device design. In particular, it can reduce the group velocity of radiation propagation [16].

The aim of this work was to study the spectral characteristics of groups of 2D PC resonant cavities with electromagnetic coupling and to determine the electromagnetic wave field localization characteristics in these structures under resonance conditions.

1. Geometry of PC Resonant Cavity and Numerical Modeling Methods

The geometry of the PC resonator is shown in Fig. 1. The PC consists of periodically arranged silicon rods with a circular cross-section of radius r and a PC lattice period a. The PC unit cell comprises one silicon rod surrounded by air. The filling factor (FF, Filling\Factor) is defined as FF $= 2r/a$. The rectangular PC resonant cavity in the PC center is formed by removing one silicon rod. The electromagnetic wave is launched into and out of the resonant cavity via PC waveguides. Reflectors made of silicon rods with radius R are positioned at the ends of the PC waveguides adjacent to the resonant cavity. The PC parameters are presented in the table. These parameters were chosen based on preliminary optimization of the PC geometry.

In numerical modeling, harmonic equations for the electric field E and magnetic field H of the electromagnetic wave were solved:

$$\nabla \times (\mu^{-1} \nabla \times E) - \omega^2 \varepsilon_c E = 0,$$

$$\nabla \times (\varepsilon_c^{-1} \nabla \times H) - \omega^2 \mu H = 0.$$

PC Parameters

Parameter	Value
Lattice period, a	653−768 nm
Radius of Si rods, r	$0.115a$
Radius of Si reflector rods, R	$1.5r$
Filling factor, FF	0.115−0.13
Refractive index of Si rods, n_1	1
Refractive index of Si rods, n_2	3.48

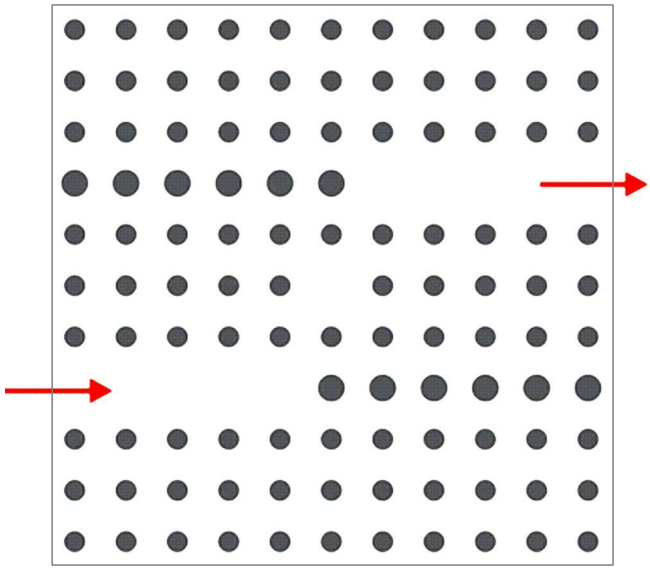

Figure 1. Geometry of a single PC resonant cavity, with input and output PC waveguides.

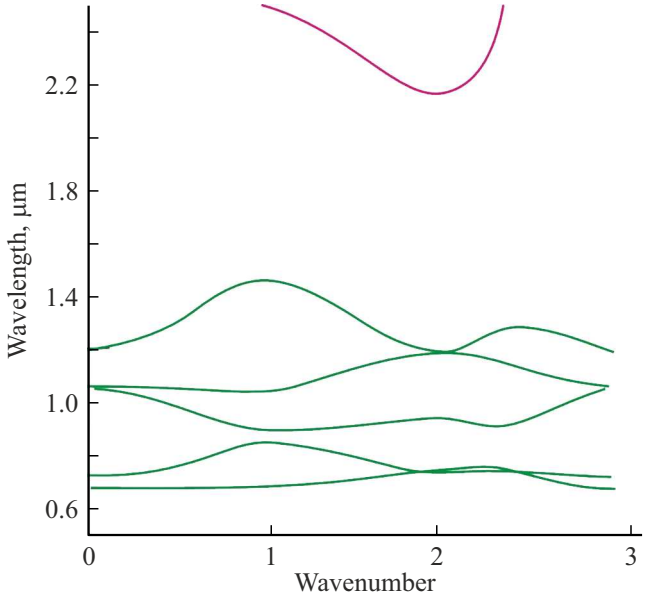

Figure 2. Photonic bandgap of the PC with parameters listed in the table. FF = 0.1156.

Here μ and ε are the magnetic permeability and dielectric permittivity, respectively, and ω is the electromagnetic wave frequency.

To ensure transparent boundaries for transmitted waves, scattered wave boundary conditions were applied. Transparency conditions were met for:

$$E = E_{sc}e^{-jk(n\cdot r)} + E_0 e^{-jk(k\cdot r)}$$

— planar scattered waves,

$$E = E_{sc}\frac{e^{-jk(n\cdot r)}}{\sqrt{r}} + E_0 e^{-jk(k\cdot r)}$$

— cylindrical scattered waves,

$$E = E_{sc}\frac{e^{-jk(n\cdot r)}}{r_s} + E_0 e^{-jk(k\cdot r)}$$

— spherical scattered waves.

Here n, k and r denote the refractive index, wave number, and radius, respectively.

Numerical simulations were performed using the FDTD method with COMSOL 5.5 Multiphysics near the wavelength 1.5 μm. The photonic band structure of the PC surrounding the waveguide was calculated using Bloch function methods. An „extremely fine“ free triangular mesh was used.. ARPACK FORTRAN routines based on the Arnoldi iteration method (IRAM) solved the formulated problems.

2. Results and discussion

2.1. Single PC Resonant Cavity

Fig. 2 shows the photonic bandgap of the PC with parameters from the table. The photonic bandgap ranges from 1.4 μm to 2.1 μm. Fig. 3 depicts the E-component distribution of the electromagnetic field (TE mode) in a single rectangular PC resonant cavity under resonance. The electromagnetic wave field is mainly concentrated at the resonant cavity center. The relative electromagnetic field intensity enhancement reaches 10.

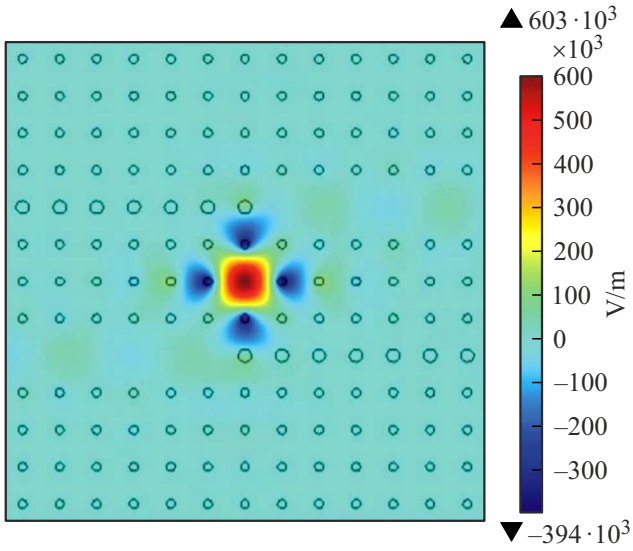

Figure 3. Distribution of the E-component of the electromagnetic field (TE mode) in a single rectangular PC resonant cavity. FF = 0.1156.

Fig. 4 presents the spectral transmission and reflection dependencies of a single PC resonant cavity. The resonance appears at a wavelength of 1.55 μm. Transmission through the resonant cavity and waveguides at this wavelength is approximately 80%. The half-width of the resonance band

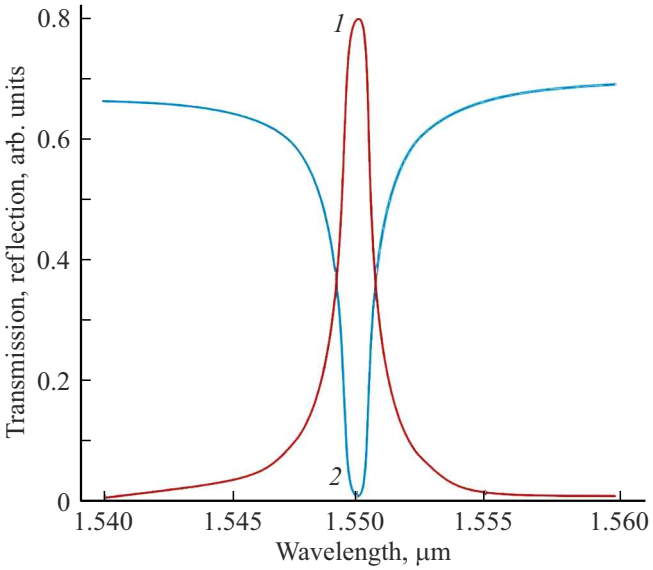

Figure 4. Spectral dependencies of transmission (*1*) and reflection (*2*) for a single PC resonant cavity. FF = 0.1156.

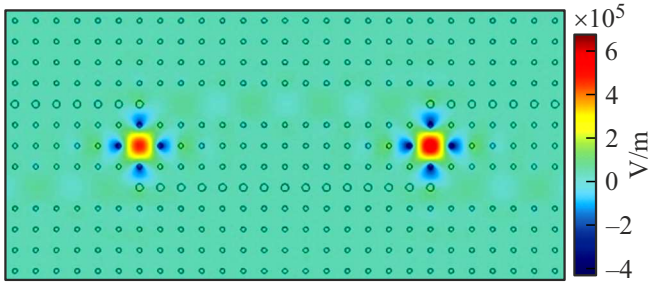

Figure 5. Distribution of the *E*-component of the electromagnetic field (TE mode) in two coupled rectangular PC resonant cavities. FF = 0.1156.

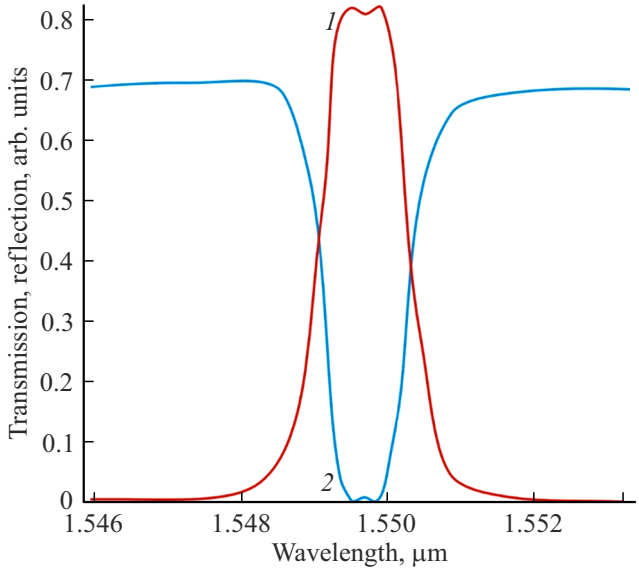

Figure 6. Spectral dependencies of transmission (*1*) and reflection (*2*) for two coupled PC resonant cavities. FF = 0.1156.

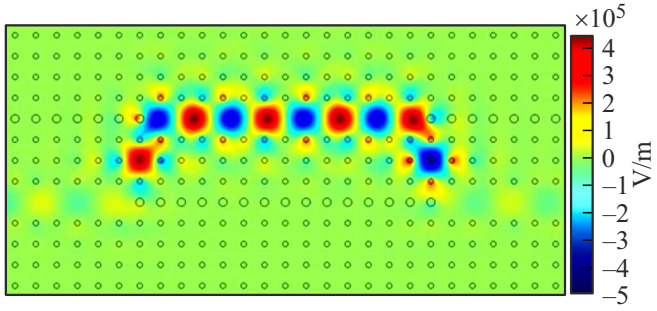

Figure 7. Distribution of the *E*-component of the electromagnetic field (TE mode) in two coupled rectangular PC resonant cavities. FF = 0.13.

is 1.5 nm. The resonant cavity quality factor reaches 1040. This allows usage of such a resonant cavity as a narrowband filter in integrated optical devices.

2.2. Two Electromagnetically Coupled PC Resonant Cavities

Fig. 5 shows the distribution of the *E*-component of the electromagnetic field for the TE mode in two coupled resonant cavities. The central PC waveguide mediating electromagnetic coupling consists of 13 elementary PC cells. Electromagnetic interaction between resonators is due to the presence of forward and backward electromagnetic waves in the central PC waveguide: forward — from the first resonant cavity to the second, and backward from the second to the first. The figure shows that the relative enhancement of the electromagnetic field intensity in the resonant cavities reaches 30, indicating that coupled rectangular resonant cavities can be useful for field enhancement in Raman scattering-based sensors. Furthermore, field localization in the second resonant cavity is stronger than in the first, with electromagnetic waves in both resonant cavities oscillating in phase.

The transmission and reflection spectra for the system of two coupled resonant cavities are shown in Fig. 6. The transmission band near resonance exhibits a flat-top profile with a small dip at the center. This feature arises from electromagnetic interaction between the two oscillatory systems: the first resonant cavity affects the second and vice versa, causing oscillation perturbations in each resonant cavity. This interaction results in the emergence of Fano resonances [17–21]. The half-width of the resonance band is 12 nm. The quality factor of the two-resonator system is 130. Such a P-shaped transmission band can be useful for the development of certain types of filters in integrated optics.

With an increase in the filling factor to FF = 0.13, the electromagnetic interaction between the two resonant cavities also increases (Fig. 7). Field localization of the

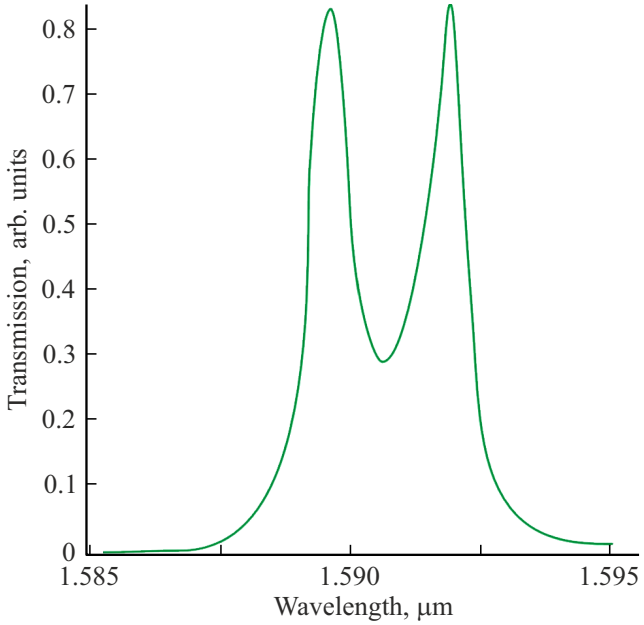

Figure 8. Spectral dependencies of transmission (*1*) and reflection (*2*) for two coupled PC resonant cavities. FF = 0.13.

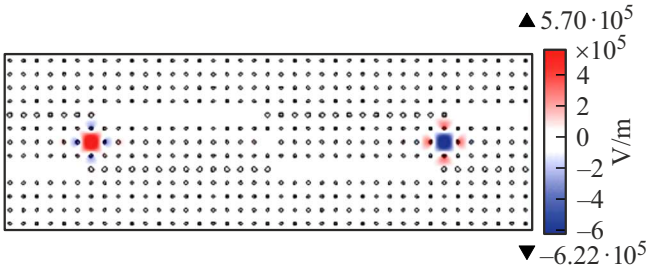

Figure 9. Distribution of the *E*-component of the electromagnetic field (TE mode) in two coupled rectangular PC resonant cavities. FF = 0.1156.

electromagnetic field in the PC waveguide between the resonant cavities is enhanced. The figure shows that the electromagnetic field in the two resonant cavities has opposite phases. The increased electromagnetic interaction between the resonant cavities leads to enhanced Fano resonance effects (Fig. 8). The dip at the center of the transmission resonance band deepens. The half-width of the resonance band in this case is 3.5 nm. The quality factor of the two coupled resonant cavity system reaches 320.

2.3. Three Electromagnetically Coupled PC Resonant Cavities

The distribution of the *E*-component of the electromagnetic field for the TE mode in a system of three electromagnetically coupled resonant cavities is shown in Fig. 9. The electromagnetic field in the right and left resonant cavities exhibits opposite phases. This is due to the total length of the two central PC waveguides. Field

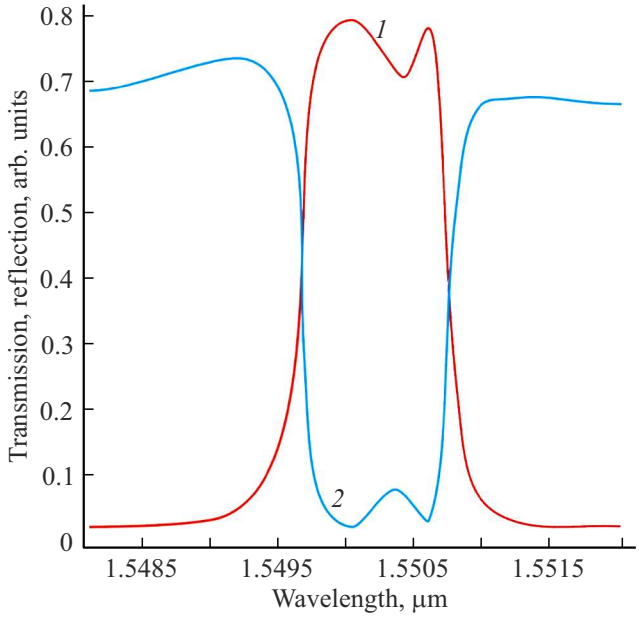

Figure 10. Spectral dependencies of transmission (*1*) and reflection (*2*) for two coupled PC resonant cavities. FF = 0.1156.

localization of the electromagnetic wave in the central waveguide is nearly zero, resulting from the summation in the central resonant cavity of forward and backward electromagnetic waves with opposite phases. The relative enhancement of the electromagnetic field intensity in the first and third PC resonant cavities reaches 15-fold.

The transmission and reflection spectra for the system of three PC resonant cavities with electromagnetic interaction are shown in Fig. 10. The transmission and reflection bands are distorted with features in the central region, indicating the emergence of Fano resonances due to electromagnetic interaction among the three coupled PC resonant cavities. The half-width of the resonance band for this system is 0.5 nm. The quality factor of the system reaches 3000.

Conclusion

Numerical modeling demonstrates that Fano resonances arise in systems of two or three 2D rectangular PC resonant cavities with electromagnetic coupling. These resonances intensify with increasing electromagnetic coupling between the resonant cavities. The electromagnetic coupling between resonant cavities increases with the filling factor. In three coupled resonant cavities, the system quality factor reaches 3000. Under resonance conditions, strong localization of the electromagnetic field intensity occurs in the resonant cavities. The relative field intensity enhancement can reach 30-fold. The described effects can be utilized in integrated optical devices, chemical and biosensors, and optical filters.

Funding

This research was supported by the „Priority 2030“ program.

Conflict of interest

The authors declare that they have no conflict of interest.

References

[1] J.D. Joannopoulos, R.D. Meade, J.N. Winn. Photonic Crystals, Molding the Flow of Light, Princeton Academic Press, Princeton, NY, (1995).
[2] R. Ferrini, D. Leuenberger, R. Houdre, H. Benisty, M. Kamp, A. Forchel. Appl. Phys. Lett., **76**, 532–537 (2000). DOI: 10.1364/OL.31.001426
[3] H. Alipour-Banaei, F. Mehdizadeh. Digest J. Nanomat. and Biostruct., **20**, 361–367 (2012).
[4] X. Zhang, Q. Liao, T. Yu, N. Liu, Y. Huang. Opt. Comm., **285**, 274–276 (2012). DOI: 10.1080/03772063.2016.1217175
[5] A. Sharkawy, S. Shi, D.W. Prather. Opt. Expr., **10**, 1048–1059 (2002). DOI: 10.1364/oe.10.001048
[6] P. Andalib, N. Granpayeh. J. Opt. Soc., **26**, 10–16 (2009). DOI: 10.1364/JOSAB.26.000010
[7] M.F.O. Hameed, M. Abdelrazzak, S.S.A. Obayya. IEEE J. Lightwave Techn., **31**, 81–86 (2013). https://opg.optica.org/jlt/abstract.cfm?URI=jlt-31-1-81
[8] C. Kang, C. Phare, S.M. Weiss. Proc. Intern. Conf. on Laser, Electro-Optics and Quant. Electr. and Laser Sci., **16**, 1–2 (2010).
[9] S. Mandal, J. Goddard, D. Erickson. Proc. Intern. Conf. on Laser, Electro-Optics and Laser Sci., **18**, 1–2 (2008).
[10] C. Lee, R. Radhakrishnan, C.-C. Chen, J. Li, J. Thillaigovindan, N. Balasubramanian. J. Lightwave Techn., **26**, 839–846 (2008). https://opg.optica.org/jlt/abstract.cfm?URI=jlt-26-7-839
[11] A. Hocini, A. Harhouz. J. Nanophot., #10, 7–12 (2016). DOI: 10.1117/1.JNP.10.016007
[12] A.I. Sidorov, Yu.O. Vidimina,. Opt. Spectr., **130**, 1185–1189 (2022). DOI: 10.21883/EOS.2022.09.54840.3355-22
[13] S. Mandal, X. Serey, D. Erickson. Nano Lett., #10, 99–104 (2010). DOI: 10.1021/nl9029225
[14] C. Monat, P. Domachuk, B.J. Eggleton. Nat. Photonics, **1**, 106–114 (2007). DOI: 10.1038/nphoton.2006.96
[15] M.I. Stockman, Electromagnetic theory of SERS. In: K. Kneipp, M. Moskovits, H. Kneipp (eds.) Surface-enhanced Raman scattering, Springer, NY, (2006).
[16] H. Altuga, J. Vučkovic. Appl. Phys. Lett., **84**, 161–163 (2004). https://opg.optica.org/abstract.cfm?URI=IQEC-2004-IThI2
[17] U. Fano. Phys Rev., **13**, 1866–1875 (1961).
[18] D.M. Riffe. Phys. Rev. B, **84**, 064308 (2011). DOI: 10.1103/PhysRevB.84.064308
[19] Y.S. Joe, A.M. Satanin, C.S. Kim. Physica Scripta, **74**, 259–266 (2006). DOI: 10.1088/0031-8949/74/2/020
[20] M.F. Limonov, M.V. Rybin, A.N. Poddubny, Y.S. Kivshar. Nature Photonics, **11**, 543–554 (2017). DOI: 10.1038/nphoton.2017.142
[21] J. Ly, Y. Ren, D. Wang, J. Wang, X. Lu, Y. Yu, W. Li, Q. Liu, X. Xu, W. Liu, P.K. Chu, C. Liu. Opt. Expr., **32**, 28334–28347 (2024). DOI: 10.1364/OE.530788

Translated by J.Savelyeva